COMPARISON OF THE DEFORMATIONS OF BRAIN TISSUES CAUSED BY TUMOR IN SEIZURE AND NON-SEIZURE PATIENTS

Julien Dauguet[1,2]*, Simon K. Warfield*[2]*, Edward Bromfield*[1]*, Alexandra Golby*[3] *and Jong Woo Lee*[1]

[1]Brigham and Women's Hospital, Department of Neurology, Boston, MA, USA
[2]Children's Hospital, Computational Radiology Laboratory, Boston, MA, USA
[3]Brigham and Women's Hospital, Department of Neurosurgery, Boston, MA, USA

ABSTRACT

It is unclear why some patients with brain tumors present with seizures while others do not. As deformations of the brain due to the tumor growth are suspected to be in part responsible for seizures, we decided to compare the differences between the brain deformations in patients presenting with seizures versus those who did not. We modeled the brain deformations by estimating the non-linear transformation which registers the postoperative image - assumed to represent the normal brain - to the preoperative image - representing the brain deformed by the tumor - on a dataset of 19 brain tumor patients. We then estimated the determinant of the Jacobian of the corresponding deformation field and built histograms of the distribution of the deformations for each image. Statistical tests performed on the histograms of seizure and non-seizure patients led to some significant differences suggesting that a higher ratio of tissue compression could be the cause of seizures.

Index Terms— Registration, Deformation, Tumor, Seizure, Statistics.

1. INTRODUCTION

Seizures are encountered in 50%-80% of patients with primary brain tumors [1]. The mechanism of epileptogenesis in tumors is incompletely understood, and is believed to be multifactorial. Low grade, well differentiated gliomas have the highest incidence of seizures. Tumors located in the limbic/temporal lobe and primary or secondary motor/sensory cortices are particularly epileptogenic [2]. The presence of seizures is only in part explained by the grade and location of the tumor. It is believed that seizures in most patients with brain tumors are caused by induced changes in the peritumoral cortex. In order to try to further determine why some patients with brain tumors present with seizures while others do not, we propose to analyze the deformation of the brain induced by the tumor. We used the information provided by the transformation field corresponding to the elastic registration of the preoperative to the postoperative MRI scans.

2. MATERIAL AND METHODS

2.1. Patients database

A database of 19 brain tumor patients who underwent ablation surgery was studied, 12 of which were presenting with seizures and the remaining 7 not. The location and the size of the tumor in the database was random and was considered to be equally distributed. A structural MRI scan at 1.5T (General Electric Medical Systems, Waukesha, WI) before ("preop" image) and after ("postop" image) the surgery were available for all of the patients in the database. The preop scans were representing the brain deformed by the tumor, whereas the postop image after complete or partial ablation of the tumor was assumed to be the state of the brain freed from the deformations causing seizure. The size of the images processed was typically $128 \times 128 \times 60$ with a typical resolution of $1.5 \times 1.5 \times 3mm$ for the postop images and $256 \times 256 \times 128$ for the preop image with a $0.9 \times 0.9 \times 1.3mm$ resolution.

2.2. Registration strategy

For each patient, a rigid then affine registrations using the blockmatching were performed for initialization. On the images registered using affine transformation, pairs of corresponding landmarks (about 100 pairs of points) were selected by a neurologist around the tumor and everywhere else in the brain (1). From these lists of corresponding points, the Thin Plate Spline transformation matching exactly the corresponding points and interpolating anywhere else the deformation field was estimated for each preop image. For each component function of the deformation field, this transformation minimizes the so-called bending energy defined as the integral over R^2 of the squares of the second derivatives. This estimation has a closed-form solution.

From this expert-based manual initialization, a cubic B-splines transformation was estimated between the manually deformed preop image and the postop image. The mutual information was used as similarity criterion as described in [3], using closed-form expressions for the criterion and its gradient. Two levels of pyramid strategy both in terms of image

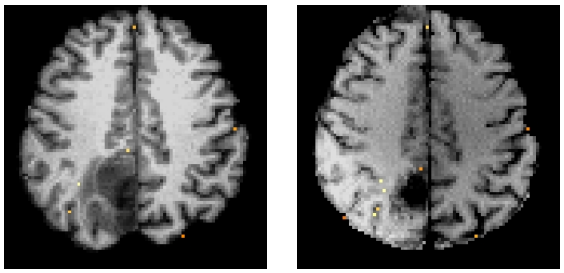

(a) (b)

Fig. 1. Corresponding landmarks (color dots) on pre-operative image (a) and post-operative image (b).

resolution as well as in terms of density of control points, were used: downsampling of the images by a factor of 2 in every direction with a $5 \times 5 \times 5$ grid of control points at pyramid level 1, and use of full resolution with a $10 \times 10 \times 10$ grid of control points at level 0. A subsample of 10% of the total number of voxels for each image was used for the computation of the joint histogram. The deformation field resulting from the composition of the manual thin plate spline transformation and the cubic B-spline transformation was computed. The image of the determinant of the jacobian J ("detjacob" image) of the resulting deformation field F in each voxel of coordinates (x_0, y_0, z_0) defined as:

$$|J(x_0, y_0, z_0)| = \left| \begin{array}{ccc} \frac{\partial F_x}{\partial x} & \frac{\partial F_x}{\partial y} & \frac{\partial F_x}{\partial z} \\ \frac{\partial F_y}{\partial x} & \frac{\partial F_y}{\partial y} & \frac{\partial F_y}{\partial z} \\ \frac{\partial F_z}{\partial x} & \frac{\partial F_z}{\partial y} & \frac{\partial F_z}{\partial z} \end{array} \right|_{(x_0,y_0,z_0)}$$

was then estimated. The mask of the brain excluding the tumor which was previously delineated on the preop image by a neurologist was applied to the detjacob image to keep the values of the deformations everywhere inside the brain except in the tumor.

2.3. Statistical tests

A normalized histogram of the masked detjacob image was then computed for each patient. Only determinant values between 0.2 and 1.3 were kept and the interval was divided into 20 bins. Patients were then sorted into 2 groups, depending on whether they had seizures or not (information on the patients symptoms were collected *a priori*). The Hotelling's T-square statistic, which is a generalization of Student's T statistic used in multivariate hypothesis testing, was performed on a sub-part of the histograms of patients between the groups. Student T-tests were also performed on each of the 20 values of the normalized histograms assuming unpaired values, homoskedasticity, and the greater, less or two-sided hypothesis. The distributions of all the values of all the detjacob images were also compared in the seizure and non-seizure groups using the Kolmogorov-Smirnov test. This latter statistical tool is a general non-parametric method for determining whether two underlying one-dimensional probability distributions differ from one another. Random sub-sets from the global distribution were also extracted in each group and compared again using Kolmogorov-Smirnov to avoid over statistical power induced by very large datasets.

3. RESULTS

3.1. Transformations

The rigid plus affine registration performed as initialization provided a decent matching of the structures but failed to capture the deformations of the brain due to the tumor, which are highly non-linear (see **Figure 2 (a), (d)**). The landmarks selected on both images were located around the tumor and close to the regions with high intensity gradient corresponding mainly to interfaces between structures. The result of the application of the elastic thin plate spline transformation computed from the list of paired points gave a good global deformation of the preop brain to match the postop brain, especially around the tumor with high deformations (see **Figure 2 (b), (d)**). However, the regions with no landmark were approximately matched and the precision of matching was limited and was operator dependent. The final cubic B-spline transformation, which was estimated automatically, provided a final refinement in the matching of structures and captured reliably most of the deformations due to the tumor expansion within the brain (see **Figure 2 (c), (d)**). The final transformation resulting from the composition of the manual thin plate splines and automatic cubic B-splines transformations looked smooth and realistic, as can be assessed on the deformed grid (see **Figure 2 (e)**). The determinant of the jacobian image of the resampling field showed inversed values compared to the transformation field as the resampling field went from the target image to the source image. A determinant of the jacobian of 1 means the transformation did not induce local volume changes. The strict positivity of the jacobian almost everywhere demonstrated that the estimated deformation did not introduce topological abberations (see **Figure 2 (f)**). Values were greater than 1 in the vicinity of the masked tumor (red regions) but were inferior to 1 almost everywhere else in the brain (all green and blue region). This distribution of values suggested that the tumor growth compressed tissues and induced contraction of a large area outside of the direct tumor vicinity.

3.2. Hotelling and Student T-test

Most of the values of the determinant of the jacobian images inside the brain were included in the interval [0.2-1.3] for the whole dataset. We thus computed the histograms of the detjacob image using these extreme values and a binning of 20 segments. The mean histogram for the seizure patients group

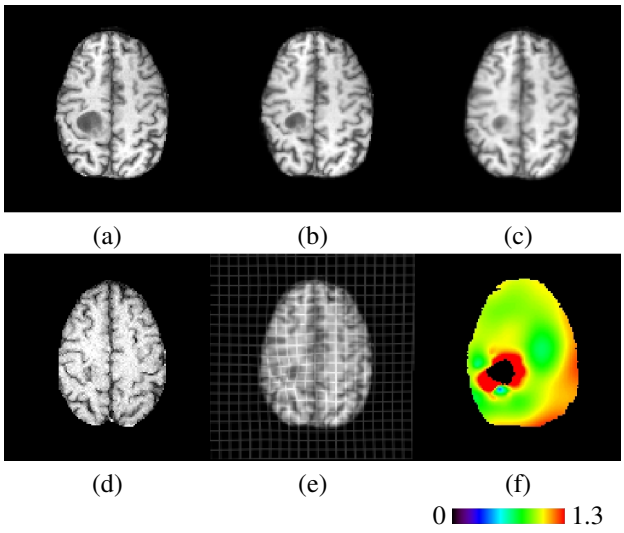

Fig. 2. Deformed pre-operative image after application of the affine transformation (a), the thin plate splines transformation estimated from manually selected landmarks (b) and the automatically calculated cubic B-splines transformation (c) to match the target post-operative image (d). A grid deformed by the composition of the 2 non-linear deformations superimosed on the transformed pre-operative image (e) and the determinant of the jacobian of the corresponding resampling field (f), after the tumor was masked out (black hole).

looked different from the non-seizure patients histogram: values were globally shifted left suggesting a higher distribution of deformations corresponding to compressed tissues (see **Figure 3**).

The Hotelling test performed on 5 consecutive bin values of the histograms between 0.74 and 1.1 - where the differences were more obvious - did not show significant differences between groups ($p - value = 0.33$). However, out of the 20 Student T-tests performed on each of the single values of the binned histogram, 2 were significant with "greater" mean assumption (preop values are globally greater than postop values), 2 again with the "less" mean assumption (preop values are globally less than postop values) and 1 with the "two-sided" assumption (see **Figure 4**). They all confirmed a tendency of the seizure patients group to have more regions with compressed tissues.

3.3. Kolmogorov-Smirnov test

The Kolmogorov-Smirnov test was performed on the 2 groups to compare the cumulative distributions of all the values of all the detjacob images. When looking at the plots of the cumulative distributions, we can see differences between the deformations in the 2 groups (see **Figure 5 (a)**). Again, the seizure group distribution is more concentrated on smaller values suggesting a higher rate of compressed tissues compared to the non-seizure group. The result of the test con-

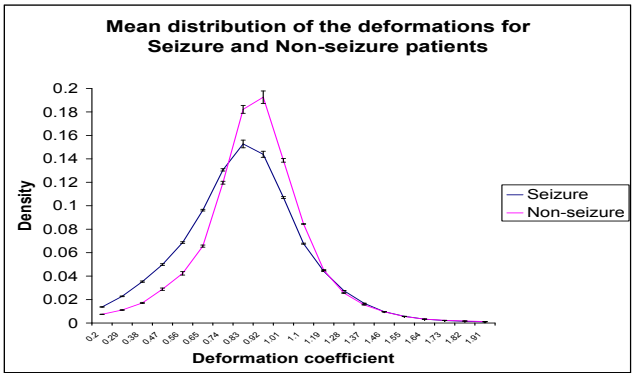

Fig. 3. Distribution histogram of the deformation coefficient in every voxel (1 means no volume variation) for all the seizure patients (blue) versus all non-seizure patients (pink) estimated on the resampling field used to register the preoperative image onto the postoperative image.

firmed highly significant differences ($p-value < 2.2e-16$). This very high significance is partly explained by the large number of values (millions of values) used to estimate the cumulative distribution in each group. To reduce the statistical power induced by the use of all the values, we randomly extracted subsets of 1000 values in each group and performed the Kolmogorov-Smirnov test again. The plots with fewer values looked similar and the statistical difference between groups found using all the values was confirmed using 10 random subsets (see **Figure 5 (b)**).

4. DISCUSSION

Because the postop images were acquired right after the surgery; whether there was not enough time for the brain to recover entirely a stable shape warrants consideration. However, most of the changes were present immediately after resection, as we were able to verify on another late postop image available for some patients. Moreover, in some cases, because of the difficult location or nature of the tumor, the resection performed was only partial. The postop image was thus not completely representative of the brain entirely freed from any deformation due to the tumor. The deformations corresponding to the apparition of the tumor were not only mechanical, in particular in the tumor region where cells' growth were pushing surrounding tissues. This is thus not the typical framework for classical registration tools. That is why we chose to perform a manual selection of landmarks by an expert to initialize the transformation prior to the use of more classical automatic registration techniques.

For this manual step, we chose to use thin plate spline transformations to model the deformations corresponding to the matching of manually selected landmarks since they were flexible enough to provide exact interpolation at irregularly distributed selected landmarks locations and they allowed a

Deformation	GREATER P-value	LESS P-value	TWO-SIDED P-value
0,2	0,15	0,85	0,31
0,29	0,08	0,92	0,17
0,38	0,06	0,94	0,11
0,47	0,07	0,93	0,14
0,56	**0,05**	0,95	0,09
0,65	**0,02**	0,98	**0,03**
0,74	0,24	0,76	0,49
0,83	0,85	0,15	0,3
0,92	0,95	0,05	0,1
1,01	0,97	**0,03**	0,06
1,1	0,96	**0,04**	0,09
1,19	0,55	0,45	0,9
1,28	0,37	0,63	0,75
1,37	0,38	0,62	0,76
1,46	0,49	0,51	0,99
1,55	0,46	0,54	0,93
1,64	0,5	0,5	0,99
1,73	0,56	0,44	0,88
1,82	0,68	0,32	0,64
1,91	0,68	0,32	0,65

Fig. 4. Results of the Student T-test performed on each of the 20 bins dividing the deformation range [0.2-1.3] of the seizure patients group vs non-seizure patients groups with the greater, less and two-sided assumptions.

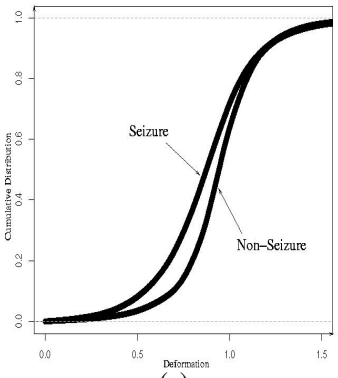

(a)

Sample	Distance	p-value
1	0.174	1.42e-13
2	0.195	2.20e-16
3	0.178	3.48e-14
4	0.159	2.10e-11
5	0.200	2.20e-16
6	0.133	4.16e-08
7	0.176	7.05e-14
8	0.172	2.84e-13
9	0.208	2.20e-16
10	0.193	2.20e-16

(b)

Fig. 5. (a): Cumulative distribution of all the deformation values for all the images of the determinant of the jacobian of the deformation field for seizure and non-seizure patients.(b): Results of the Kolmogorov-Smirnov test performed on 10 random samples of 1000 values of the determinant of the jacobian comparing the seizure and the non-seizure groups.

realistic (based on a mechanical model) interpolation elsewhere. After this step, corresponding structures were moved closer and the biggest deformations were strongly reduced. We then chose to use cubic B-splines to refine the transformation, since it guaranteed a flexible but smooth (although not always invertible) deformation based on a regularly distributed grid.

Comparing the deformations of a group of patients with the tumor in very different location, with a different size, shape and nature was not an easy task. In particular, SPM-like approaches, where all the subjects are spatially normalized onto a template and the detjacob images are compared to find clusters of voxels with significant differences in gray levels, were not applicable. We decided to compare the normalized distribution of the determinant of the jacobian - which represents the local variation of volume induced by the deformation, and therefore gives an idea of the compression/extension of tissue - between groups. After masking out the region of the tumor in the determinant of the jacobian image, the normalized histograms of this quantity were neither depending on the tumor location, size, nature nor the image size, which allows a valid comparison between patients.

The Hotelling test performed on the histogram values between groups was not significant, although differences could be expected between mean histogram plots. This non-significance was probably due to the relatively small number of patients in each group (12 vs 7) compared to the number of values tested (10). Note that we could not perform the test on all of the 20 values because we only had 19 patients in total. The significant differences which were found with the individual Student T-tests, and with the Kolmogorov-Smirnov tests on all the values or on random subsets of values, demonstrated that brain tissues were more compressed in seizure patients brains compared to non-seizure. This result could therefore be interpreted as a strong indication that seizures are caused by brain tissues being too much compressed by the development of the tumor causing disturbances of underlying neuronal functions.

We showed in this study that brain tumor patients presenting seizure symptoms had a higher rate of compressed tissues compared to non-seizure patients. This result is original and is a novel application of the use of elastic deformations in neurological studies and of what can be learned from computational medicine.

5. ACKNOWLEDGMENTS

This investigation was supported by a grant from the National Epifellows Foundation and in part by NIH grants R03 CA126466, R01 RR021885, R01 GM074068, R01 EB008015 and NSF ITR 0426558.

6. REFERENCES

[1] J. Hildebrand, C. Lecailleand J. Perennes, and J.Y. Delattre, "Epileptic seizures during follow-up of patients treated for primary brain tumors," *Neurology*, vol. 65, pp. 212–15, 2005.

[2] F.T. Vertosick, R.G Selker, and V.C. Arena, "Survival of patients with well-differentiated astrocytoma diagnosed in the era of computed tomography," *Neurosurgery*, vol. 28, pp. 496–501, 1991.

[3] D. Rueckert, C. Hayes, C. Studholme, P. Summers, M. Leach, and D. J. Hawkes, "Non-rigid registration of breast MR images using mutual information," *LNCS*, vol. 1496, pp. 1144–52, 1998.